Foxr1 is a novel maternal-effect gene in fish that is required for early embryonic success

Caroline Cheung, Amélie Patinote, Yann Guiguen, Julien Bobe

foxr1 is a novel maternal-effect gene in fish that is required for early embryonic success

Caroline T. Cheung, Amélie Patinote, Yann Guiguen and Julien Bobe

LPGP, UR1037 Fish Physiology and Genomics, INRA, Rennes, France

ABSTRACT

The family of forkhead box (Fox) transcription factors regulates gonadogenesis and embryogenesis, but the role of *foxr1* in reproduction is unknown. Evolutionary history of *foxr1* in vertebrates was examined and the gene was found to exist in most vertebrates, including mammals, ray-finned fish, amphibians, and sauropsids. By quantitative PCR and RNA-seq, we found that *foxr1* had an ovarian-specific expression in zebrafish, a common feature of maternal-effect genes. In addition, it was demonstrated using in situ hybridization that *foxr1* was a maternally-inherited transcript that was highly expressed even in early-stage oocytes and accumulated in the developing eggs during oogenesis. We also analyzed the function of *foxr1* in female reproduction using a zebrafish CRISPR/cas9 knockout model. It was observed that embryos from the *foxr1*-deficient females had a significantly lower survival rate whereby they either failed to undergo cell division or underwent abnormal division that culminated in growth arrest at around the mid-blastula transition and early death. These mutant-derived eggs contained dramatically increased levels of *p21*, a cell cycle inhibitor, and reduced *rictor*, a component of mTOR and regulator of cell survival, which were in line with the observed growth arrest phenotype. Our study shows for the first time that *foxr1* is an essential maternal-effect gene and may be required for proper cell division and survival via the p21 and mTOR pathways. These novel findings will broaden our knowledge on the functions of specific maternal factors stored in the developing egg and the underlying mechanisms that contribute to reproductive success.

Submitted 11 April 2018
Accepted 8 August 2018
Published 23 August 2018

Corresponding author
Julien Bobe, Julien.Bobe@inra.fr

Academic editor
Mason Posner

Additional Information and Declarations can be found on page 17

DOI **10.7717/peerj.5534**

Subjects Aquaculture, Fisheries and Fish Science, Cell Biology, Developmental Biology, Evolutionary Studies, Genetics

Keywords CRISPR-cas9, Maternal-effect genes, *foxr1*, p21, Cell growth and survival, Rictor, Zebrafish, Egg quality

INTRODUCTION

In vertebrates, maternal products including transcripts, proteins, and other biomolecules are necessary for initiating early embryonic development from fertilization until the mid-blastula transition (MBT) when the zygotic genome is activated (*Baroux et al., 2008*). Maternal-effect genes are transcribed from the maternal genome and encode the maternal factors that are deposited into the developing oocytes in order to coordinate embryonic development before MBT (*Lindeman & Pelegri, 2010*). We had previously explored the zebrafish egg transcriptome (*Cheung et al., 2018*) and proteome (*Yilmaz et al., 2017*) in order to gain further understanding of the maternal factors that contribute to

good quality or developmentally competent eggs that result in high survival of progeny. However, despite the increasing identification of maternal-effect genes and their functions, large gaps still remain especially the role of genes that regulate early embryogenesis.

The forkhead box (Fox) proteins belong to a family of transcription factors that play important roles in cell growth, proliferation, survival, and cell death (*Hannenhalli & Kaestner, 2009*). Many of these Fox proteins have been shown to be essential to the various processes of embryogenesis. In mammals, knockouts of several *fox* genes, including *foxa2*, *foxo1*, and *foxf1*, result in embryonic lethality due to defects in development of different organs (*Hannenhalli & Kaestner, 2009*; *Martins, Lithgow & Link, 2016*; *Mahlapuu et al., 2001*). In reproduction, a recent transcriptomic study in the Nile tilapia, *Oreochromis niloticus*, showed that more than 50 *fox* genes were expressed in the gonads, and some of these, including *foxl2*, *foxo3*, and *foxr1* (formerly known as *foxn5*), were specific to XX females (*Yuan et al., 2014*). *foxl2* and its relatives are known to be key players in ovarian differentiation and oogenesis in vertebrates. Foxl2 is essential for mammalian ovarian maintenance, and it was demonstrated in Nile tilapia, medaka, and zebrafish that *foxl2* is also a critical regulator of ovary development and maintenance (*Bertho et al., 2016*). Further, *foxo3* was shown to be required for ovarian follicular development, and its knockout in mice led to sterility in female mutants due to progressive degeneration of the developing oocytes and lack of ovarian reserve of mature oocytes (*Hosaka et al., 2004*). *foxr1* was also found to have sexually dimorphic expression in eels (*Anguilla anguilla* and *Monopterus albus*) and marine medaka (*Oryzias melastigma*), and was predominately observed in the ovaries (*Geffroy et al., 2016*; *Chi et al., 2017*; *Lai et al., 2015*). However, despite these observational studies, the function of *foxr1* in vertebrates, especially its role in reproduction, remains unclear. Thus, in this study, we investigated the evolution of *foxr1* and its phylogenetic relationship in a wide range of vertebrate species, as well as its biological function using knockout zebrafish models created by the CRISPR/cas9 system to broaden our knowledge of the evolutionary origin of maternal-effect genes and the underlying mechanisms that contribute to reproductive success in vertebrates.

MATERIALS AND METHODS

Protein databases

Since our model is based on the zebrafish, all gene/protein nomenclatures will be based on those of fish. First, human (*Homo sapiens*) Fox protein R1 (Foxr1; ENSG00000176302) was used to BLAST for related protein sequences, and the following amino acid data were retrieved from the ENSEMBL database (http://www.ensembl.org/index.html): mouse, *Mus musculus*; rat, *Rattus norvegicus*; guinea pig, *Cavia porcellus*; pig, *Sus scrofa*; horse, *Equus caballus*; cow, *Bos taurus*; panda, *Ailuropoda melanoleuca*; opossum, *Monodelphis domestica*; Chinese softshell turtle, *Pelodiscus sinensis*; armadillo, *Dasypus novemcinctus*; frog, *Xenopus tropicalis* (Foxr1 a); fruit fly, *Drosophila melanogaster*; nematode, *Caenorhabditis elegans*; sea squirt, *Ciona intestinalis*; lamprey, *Petromyzon marinus*; coelacanth, *Latimeria chalumnae*; spotted gar, *Lepisosteus oculatus* (Foxr1 a); cod, *Gadus morhua* (Foxr1 a); fugu, *Takifugu rubripes*; medaka, *Oryzias latipes* (Foxr1 a);

platyfish, *Xiphophorus maculatus*; stickleback, *Gasterosteus aculeatus*; tetraodon, *Tetraodon nigroviridis*; tilapia, *Oreochromis niloticus*; zebrafish, *Danio rerio* (Foxn1 and Foxn3); and cave fish, *Astyanax mexicanus*. Then, the protein sequence for zebrafish (Foxr1; NP_001096594.1) was found in the NCBI database (http://www.ncbi.nlm.nih.gov). Using this amino acid sequence as bait in BLAST, the bald eagle, *Haliaeetus leucocephalu*; penguin, *Pygoscelis adeliae*; crested ibis, *Nipponia nippon*; swan goose, *Anser cygnoides domesticus*; American alligator, *Alligator mississippiensis*; Chinese alligator, *Alligator sinensis*; python, *Python bivittatus*; central bearded dragon, *Pogona vitticeps*; frog, *Xenopus laevis* and *Xenopus tropicalis* (Foxr1 b) ; medaka, *Oryzias latipes* (Foxr1 b); northern pike, *Esox lucius* (Foxr1 a); rainbow trout, *Oncorhynchus mykiss* (Foxr1 a); coho salmon, *Oncorhynchus kisutch*; and Atlantic salmon, *Salmo salar*, protein sequences were extracted and investigated from the NCBI database. Further, using the protein sequence for zebrafish Foxr1, the following protein sequences were extracted from our previously established PhyloFish online database (http://phylofish.sigenae.org/index.html) (*Pasquier et al., 2016*) and analyzed along with the others: spotted gar, *Lepisosteus oculatus* (Foxr1 b); cod, *Gadus morhua* (Foxr1 b); bowfin, *Amia calva*; European eel, *Anguilla anguilla*; butterflyfish, *Pantodon buchholzi*; sweetfish, *Plecoglossus altivelis*; allis shad, *Alosa alosa*; arowana, *Osteoglossum bicirrhosum*; panga, *Pangasius hypophthalmus*; northern pike, *Esox lucius* (Foxr1 b); eastern mudminnow, *Umbra pygmae*; American whitefish, *Coregonus clupeaformis*; brook trout, *Salvelinus fontinalis* (Foxr1 a and b); rainbow trout, *Oncorhynchus mykiss* (Foxr1 b); European whitefish, *Coregonus lavaretus*; grayling, *Thymallus thymallus*; and European perch, *Perca fluviatilis*. These sequences are compiled in Data S1.

Phylogenetic analysis

The phylogenetic analysis was conducted using the Phylogeny.fr online program with default settings (*Dereeper et al., 2008*, *2010*). Amino acid sequences of 73 Foxr1, Foxr2, Foxn1, and Foxn3 proteins from the above-mentioned species were aligned using the MUSCLE pipeline, alignment refinement was performed with Gblocks, and then the phylogenetic tree was generated using the Maximum Likelihood method (PhyML pipeline) with 100 bootstrap replicates.

Synteny analyses

Synteny maps of the conserved genomic regions of *foxr1* and *foxr2* were produced with spotted gar as the reference gene using PhyloView on the Genomicus v91.01 website (http://www.genomicus.biologie.ens.fr/genomicus-91.01/cgi-bin/search.pl).

Fish husbandry

Wildtype zebrafish (*Danio rerio*) of the AB strain were maintained at 25 °C in a central filtration recirculating system with a 12 h light/dark cycle in the INRA LPGP fish facility (Rennes, France). Individual couple pairing was performed by placing a male and a female overnight in a tank with a partition for separation, and in the morning, the divider was removed after which the female released her eggs to be fertilized by the male. All procedures of fish husbandry and sample collection were in accordance with the guidelines set by the

French and European regulations on animal welfare. Protocols were approved by the Rennes ethical committee for animal research (CREEA) under approval no. R2012-JB-01.

Quantitative real-time PCR

Tissue samples from two wildtype males and three wildtype females, and 50–200 fertilized eggs at the one-cell stage from 32 wildtype couplings, which were all used as separate biological replicates, were harvested, and total RNA was extracted using Tri-Reagent (Molecular Research Center, Cincinnati, OH, USA) according to the manufacturer's instructions. The tissue and egg samples were flash-frozen in liquid nitrogen immediately upon harvest and stored at −80 °C until use. Reverse transcription (RT) was performed using one μg of RNA from each sample with the Maxima First Strand cDNA Synthesis kit (Thermo Scientific, Waltham, MA, USA). Briefly, RNA was mixed with the kit reagents, and RT performed at 50 °C for 45 min followed by a 5-min termination step at 85 °C. Control reactions were run without reverse transcriptase and used as negative control in the quantitative real-time PCR (qPCR) study. qPCR experiments were performed with the Fast-SYBR GREEN fluorophore kit (Applied Biosystems, Foster City, CA, USA) as per the manufacturer's instructions using 200 nM of each primer in order to keep PCR efficiency between 90% and 100%, and an Applied Biosystems StepOne Plus instrument. The StepOne software was used for expression analysis. RT products, including control reactions, were diluted 1/25, and four μL of each sample were used for each PCR. All qPCR experiments were performed in duplicate using technical replicates. The relative abundance of target cDNA was calculated from a standard curve of serially diluted pooled cDNA and normalized to *18S*, β-*actin*, and *EF1*α transcripts. We considered a Ct variation of around 0.5 as acceptable. The R^2 values for *foxr1*, *p21*, *p27*, and *rictor* were 91.69%, 90.57%, 90.03%, and 90.36%, respectively. Melting curves were used and qPCR products were sequenced for confirmation. The primer sequences can be found in Data S2. The tissue expression of *foxr1* was detected using the *foxr1* genotyping forward and reverse primers while the mutant form of *foxr1* in the CRISPR/cas9-mutated eggs was assessed with the *foxr1* qPCR forward and reverse primers.

RNA-seq

Expression profiles in different holostean and teleostean species were obtained using the publicly available PhyloFish database http://phylofish.sigenae.org/index.html. Corresponding RNA-seq data were deposited into Sequence Read Archive of NCBI under accession references SRP044781–SRP044784, SRP045138, SRP045098–SRP045103, and SRP045140–SRP045146. The construction of sequencing libraries, data capture and processing, sequence assembly, mapping, and interpretation of read counts were all performed as previously described (*Pasquier et al., 2016*). The number of mapped reads was then normalized for the *foxr1* gene across the 11 tissues using RPKM normalization.

In situ hybridization

Ovary samples were first fixed in 4% paraformaldehyde overnight, dehydrated by sequential methanol washes, paraffin-embedded, and sectioned to seven μm thickness

before being subjected to the protocol. The sections were deparaffinized and incubated with 10 μg/mL of proteinase K for 8 min at room temperature, followed by blocking with the hybridization buffer (50% formamide, 50 μg/mL heparin, 100 μg/mL yeast tRNA, 1% Tween 20, and 5X saline-sodium citrate [SSC]). The probe was diluted to one ng/μL in the hybridization buffer and incubated overnight at 55 °C in a humidification chamber. The probes were synthesized by cloning a fragment of the *foxr1* gene into the pCRII vector using the cloning *foxr1* forward and reverse primers (Data S2) and Topo TA Cloning kit (Invitrogen, Carlsbad, CA, USA) as per the manufacturer's protocol. The digoxigenin (DIG)-labeled sense and anti-sense probes were transcribed from Sp6 and T7 transcription sites, respectively, of the vector containing the cloned *foxr1* fragment and purified using 2.5M LiCl solution. The purity and integrity of the probes were verified using the Nanodrop spectrophotometer (Thermo Scientific, Waltham, MA, USA) and the Agilent RNA 6000 Nano kit along with the Agilent 2100 bioanalyzer (Santa Clara, CA, USA). The slides were then subjected to two washes each with 50% formamide/2X SSC, 2X SSC, and 0.2X SSC at 55 °C followed by two washes with PBS at room temperature. The sections were subsequently blocked with blocking buffer (2% sheep serum, 3% bovine serum albumin, 0.2% Tween 20, and 0.2% Triton-X in PBS), and the anti-DIG antibody conjugated to alkaline phosphatase (Roche Diagnostics, Mannheim, Germany) was diluted by 1/500 and applied for 1.5 h at room temperature. The sections were washed with PBS and visualized with NBT/BCIP (nitro blue tetrazolium/5-bromo-4-chloro-3-indolyl phosphate).

CRISPR-cas9 genetic knockout

CRISPR/cas9 guide RNA (gRNA) were designed using the ZiFiT (*Sander et al., 2010*; *Mali et al., 2013*) online software and were made against two targets within the gene to generate a genomic deletion of approximately 240 base pairs (bp) that spans the last exon which allowed the formation of a non-functional protein. Nucleotide sequences containing the gRNA were ordered, annealed together, and cloned into the DR274 plasmid. In vitro transcription of the gRNA from the T7 initiation site was performed using the Maxiscript T7 kit (Applied Biosystems, Foster City, CA, USA) and of the cas9 mRNA using the mMESSAGE mMACHINE kit (Ambion/Thermo Scientific, Waltham, MA, USA) from the Sp6 site, and their purity and integrity were assessed using the Agilent RNA 6000 Nano Assay kit and 2100 Bioanalyzer. Zebrafish embryos at the one-cell stage were micro-injected with approximately 30–40 pg of each CRISPR/cas9 guide along with purified cas9 mRNA. The embryos were allowed to grow to adulthood, and genotyped using fin clip and PCR that detected the area around the deleted region. The full-length wildtype PCR band was 400 bp, and the mutant band with the CRISPR/cas9-generated deletion was approximately 160 bp using the *foxr1* genotyping pair of primers. The PCR bands of the mutants were then sent for sequencing to verify the deletion. Once confirmed, the mutant females were mated with males harboring the *vasa::gfp* gene, where *vasa* was fused with *gfp* at the 3′ end, to produce F1 embryos, whose phenotypes were subsequently recorded. Images were captured with a Nikon AZ100 microscope and DS-Ri1 camera (Tokyo, Japan).

Genotyping by PCR

Fin clips were harvested from animals under anesthesia (0.1% phenoxyethanol) and lysed with 5% chelex containing 100 μg of proteinase K at 55 °C for 2 h and then 99 °C for 10 min. The extracted DNA was subjected to PCR using Jumpstart Taq polymerase (Sigma-Aldrich, St. Louis, MO, USA) and the *foxr1* forward and reverse primers that are listed in Data S2.

Statistical analysis

Comparison of two groups was performed using the GraphPad Prism statistical software (La Jolla, CA, USA), and either the Student's *t*-test or Mann–Whitney *U*-test was conducted depending on the normality of the groups based on the Anderson–Darling test. A p-value < 0.05 was considered as significant.

RESULTS

Phylogenetic analysis of Foxr1-related sequences

foxr1 and *foxr2* were formerly known as *foxn5* and *foxn6*, respectively (*Katoh & Katoh, 2004a*, *2004b*). To date, there are six reported members of the *foxr/foxn* family (*foxn1*, *foxn2*, *foxn3*, *foxn4*, *foxr1*, and *foxr2*). To examine the evolution of *foxr1*, we used a Blast search approach using the zebrafish Foxr1 protein sequence as query in various public databases to retrieve 73 protein sequences from other species that could be related to this protein. All retrieved sequences are compiled in Data S1. Of note, both Foxr1 and Foxr2 protein sequences were retrieved. In order to verify that the retrieved protein sequences (Data S1) were homologous to zebrafish Foxr1, a phylogenetic analysis was performed. Based on the alignment of the retrieved vertebrate Foxr1-related sequences, and using Foxn1 and Foxn3 amino acid sequences as out-groups, a phylogenetic tree was generated (Fig. 1). As shown in Fig. 1, the common ancestor of the vertebrate *foxr1* and *foxr2* genes diverged from the ancestor of *foxn1* and *foxn3* genes, and these sequences were clearly observed as two separate clades belonging to actinopterygii (ray-finned fish) and sarcopterygii (lobe-finned fish and tetrapods). In addition, Foxr2 was found only in mammals with no homologs detected in actinopterygii as well as sauropsids and amphibians. Remarkably, despite the wide-ranging presence of Foxr1, no related sequences were observed in invertebrates and chondrichthyans (dogfish and sharks) or in certain species such as chicken (*Gallus gallus*). On the other hand, several species showed two Foxr1 sequences including the salmonids, rainbow trout (*Oncorhynchus mykiss*) and brook trout (*Salvelinus fontinalis*), as well as northern pike (*Esox lucius*), cod (*Gadus morhua*), medaka (*Oryzias latipes*), and spotted gar (*Lepisosteus oculatus*).

In line with the previous report that stated that *foxr2* was absent in tilapia, stickleback, zebrafish, and medaka genomes, we retrieved Foxr2 protein sequences only in mammals using the zebrafish Foxr1 peptide sequence as query. Thus, using zebrafish Foxr1 sequence as the reference protein, we subsequently compared Foxr1 homology with the Foxr1 and Foxr2 sequences from mammals. As shown in Data S3, there was 29–37% identity and 41–53% similarity between all sequences, and there did not appear to be any difference in homology between zebrafish Foxr1 and mammalian Foxr1 and Foxr2 sequences.

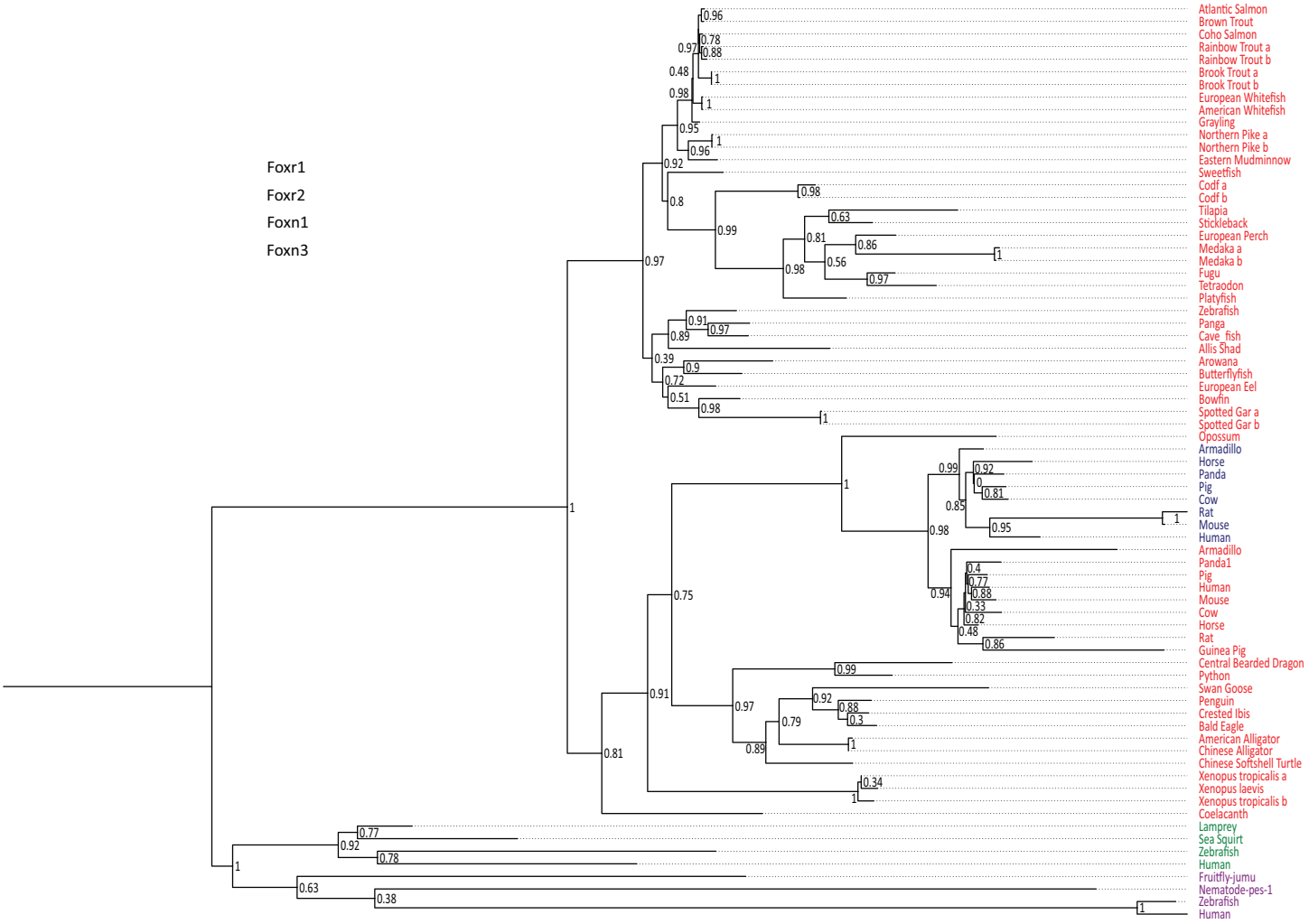

Figure 1 Phylogenetic tree of vertebrate Foxr1 and Foxr2 proteins. This phylogenetic tree was constructed based on the amino acid sequences of Foxr1 proteins (for the references of each sequence see Data S1) using the Maximum Likelihood method with 100 bootstrap replicates. The number shown at each branch node indicates the bootstrap value (%). The tree was rooted using Foxn1 and Foxn3 sequences. The Foxr1 sequences are in red, Foxr2 sequences are in blue, those of Foxn1 are in green, and Foxn3 sequences are in purple. a and b denotes multiple copies of Foxr1 sequences.
Full-size DOI: 10.7717/peerj.5534/fig-1

Further, there was 47–60% identity and 59–77% similarity between mammalian Foxr1 and Foxr2 sequences, indicating that these two proteins are highly similar and probably diverged recently during evolution.

Synteny analysis of *foxr1* and *foxr2* genes in vertebrates

In order to further understand the origin of the *foxr1* and *foxr2* genes in vertebrates, we performed a synteny analysis of their neighboring genes in representative vertebrate genomes using the basal actinopterygian, spotted gar, as the reference genome and the Genomicus online database (Fig. 2). We found that between the spotted gar and mammals, there was conserved synteny of the *foxr1*, *upk2*, *ccdc84*, *rps25*, *trappc4*, *slc37a4*, and *ccdc153* loci in their genomes. In the frog (*Xenopus tropicalis*) genome, the *foxr1*, *ccdc153*, *cbl*,

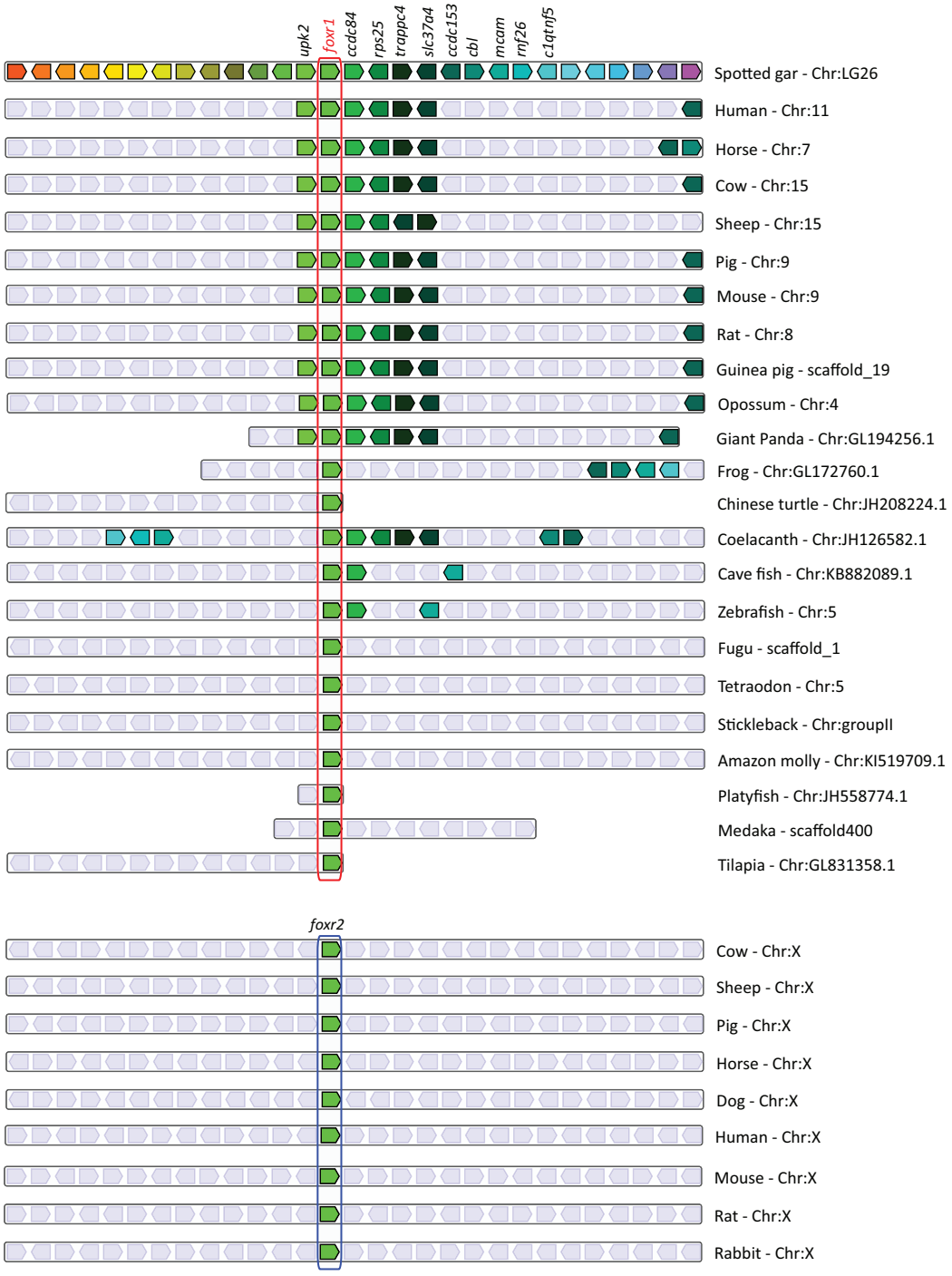

Figure 2 Conserved genomic synteny of *foxr1* genes. Genomic synteny maps comparing the orthologs of *foxr1*, *foxr2*, and their neighboring genes, which were named after their human orthologs according to the Human Genome Naming Consortium (HGNC). Orthologs of each gene are shown in the same color, and the chromosomal location is shown next to the species name. *foxr1* orthologs are boxed in red while *foxr2* orthologs are boxed in blue. Light gray boxes denote the lack of synteny of the corresponding genes in the indicated species as compared to gar. Full-size DOI: 10.7717/peerj.5534/fig-2

mcam, and *c1qtnf5* loci were conserved, while in Coelacanth, *foxr1*, *ccdc84*, *rps25*, *trappc4*, *slc37a4*, *cbl*, *ccdc153*, *mcam*, *c1qtnf5*, as well as *rnf26* loci were found in the same genomic region as those of the spotted gar. However, amongst the actinopterygians, there was lower conservation of synteny; in zebrafish and cave fish, the *foxr1*, *ccdc84*, and *mcam* loci were conserved while in the other ray-finned fish species, only the *foxr1* loci was found. We further analyzed the *foxr2* sequences that were found only in mammals, and we demonstrate here that they were all present on the X chromosome with no apparent conserved synteny of neighboring genes to those found in the spotted gar. Our overall analyses suggest that all the *foxr*-related sequences that were found were homologs, and the *foxr* gene in fish species probably derived from the ancestral *foxr1* gene. Although there was the same degree of protein homology between zebrafish Foxr1 and mammalian Foxr1 and Foxr2 sequences, the phylogenetic tree and synteny analyses showed a clear distinction between them, and the *foxr2* gene probably derived from a later single gene duplication or transposon event as previously suggested (*Katoh & Katoh, 2004a*).

Expression profiles of *foxr1*

We next focused our efforts on *foxr1* since it has previously been shown in eel, tilapia, and medaka to be gonad specific and thus may have specific functions in reproduction. In order to investigate the potential functions of *foxr1*, we explored its tissue distribution using two different approaches, qPCR and RNA-seq, the latter of which was obtained from the PhyloFish online database (*Pasquier et al., 2016*). In zebrafish, we observed from both sets of data that *foxr1* mRNA was predominantly expressed in the ovary and unfertilized egg (Figs. 3A and 3B). A high expression of *foxr1* transcript was also detected in bone by RNA-seq, but not by qPCR; this could be due to methodological differences as RNA-seq is more sensitive than qPCR since it is designed to detect the sequences all along the transcript while the latter detects just one area of the transcript. Thus, it is possible that a different splice variant of *foxr1* exists in bone. By in situ hybridization (ISH), we also demonstrated that *foxr1* transcripts were highly expressed in the ovary in practically all stages of oogenesis (Figs. 3C–3E; negative controls, Figs. 3F–3H).

Functional analysis of *foxr1* in zebrafish

To understand the role of *foxr1* during oogenesis and early development, we performed functional analysis by genetic knockout using the CRISPR/cas9 system. One-cell staged embryos were injected with the CRISPR/cas9 guides that targeted *foxr1* and allowed to grow to adulthood. Mosaic founder mutant females (F0) were identified by fin clip genotyping and subsequently mated with *vasa::gfp* males, and embryonic development of the F1 fertilized eggs was recorded. Since the mutagenesis efficiency of the CRISPR/cas9 system was very high, as previously described (*Auer et al., 2014*; *Gagnon et al., 2014*), the *foxr1* gene was sufficiently knocked-out even in the mutant mosaic F0 females. This was evidenced by the substantially lower transcript level of *foxr1* in the F1 embryos as compared to those from control pairings (0.78 ± 0.22 and 1.65 ± 0.04, respectively; Fig. 4A). Thus, the phenotypes of *foxr1* (n = 5) mutants could be observed even in the F0 generation. Since neither males nor the females could transmit the mutated genes to

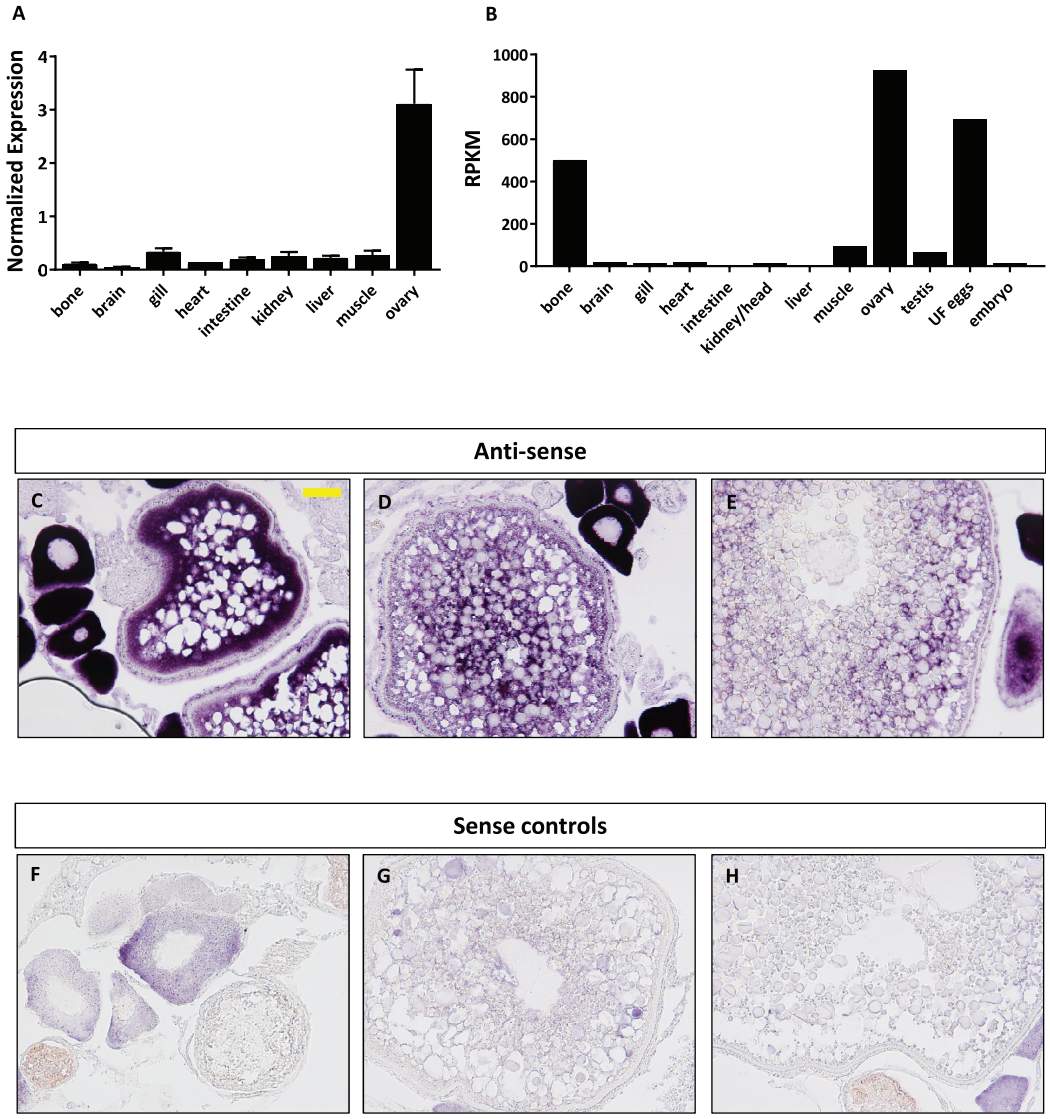

Figure 3 Expression profile of *foxr1* in zebrafish. Tissue expression analysis of *foxr1* mRNA in adult zebrafish (A) by quantitative real-time PCR (qPCR) and (B) RNA-seq. Expression level by qPCR is expressed as a normalized value following normalization using *18S*, β-*actin*, and *ef1*α expression while that by RNA-seq is expressed in read per kilobase per million reads (RPKM). Tissues were harvested from three to four wildtype zebrafish individuals. (C–H) In situ hybridization was performed for *foxr1* in zebrafish ovaries from wildtype females. Positive staining is demonstrated using the anti-sense probe against *foxr1* (Figs 3C–3E) in blue with 5-bromo-4-chloro-3-indolyl-phosphate/nitro blue tetrazolium as substrate. The negative control was performed with the sense probe (Figs 3F–3H). About 20× magnification; scale bar denotes 90 μm. $N = 5$ each for *foxr1* mutant and control. UF, unfertilized.

Full-size DOI: 10.7717/peerj.5534/fig-3

future generations (i.e. all the surviving embryos were WT), all of our observations were obtained from the F1 generation, which were the fertilized eggs derived from the mosaic female *foxr1* mutants.

We observed that most of the embryos from the *foxr1* mutant females had a very low developmental success at 24 hpf (23.2 ± 8.4% vs. 85.2 ± 9.2% in controls; $p < 0.008$)

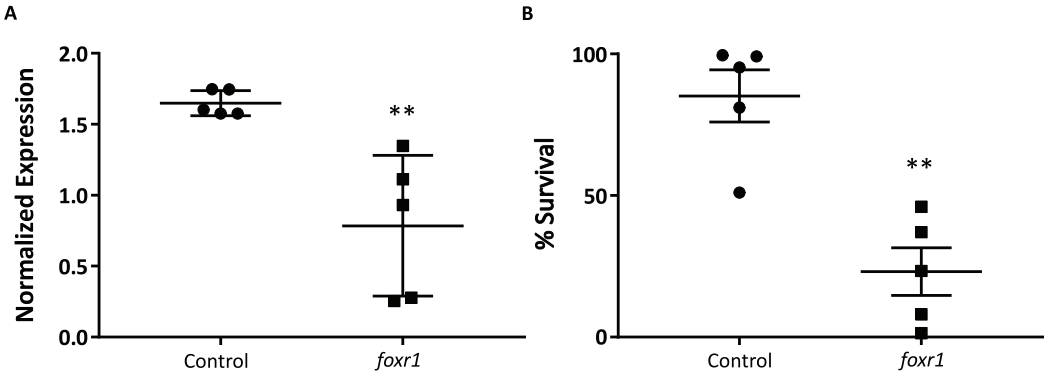

C

Frequency of *foxr1* mutant phenotypes

Individual mutant	Total number of embryos	Embryos with defects		Normal embryos	% Survival of normal embryos to total embryos
		Non-cellularized[#]	Cellularized with developmental defects[+]		
foxr1-1	517	333	0	184	36%
foxr1-2	183	183	0	0	0%
foxr1-3	212	195	0	17	8%
foxr1-4	435	194	60	201	46%
foxr1-5	268	84	80	104	39%
WT-1	478	91	0	387	81%
WT-2	297	3	0	294	99%
WT-3	223	11	0	212	95%
WT-4	256	56	0	200	78%
WT-5	196	2	0	194	99%

Figure 4 CRISPR/cas9 knockout of *foxr1* in zebrafish. (A) Normalized expression level of *foxr1* transcript by quantitative real-time PCR (qPCR) in the fertilized zebrafish eggs from crosses between *foxr1* mutant females and *vasa::gfp* males. (B) Developmental success (% survival) at 24 h post-fertilization (hpf) as measured by the proportion of fertilized eggs that underwent normal cell division and reached normal developmental milestones based on *Kimmel et al. (1995)* from crosses between *foxr1* mutant females and *vasa::gfp* males. (C) Frequency of *foxr1* mutant phenotypes in the F1 eggs between crosses of *foxr1* mutant females and *vasa::gfp* males. [#]Embryos did not develop at all (please refer to Figs 5E–5H). [+]Embryos had a partially cellularized blastodisc that was sitting atop an enlarged syncytium (please refer to Figs 5I–5L). The graphs demonstrate representative data from a single clutch from a mutant female. qPCR data were normalized to *18S*, β-*actin*, and *ef1*α. $N = 5$ each for *foxr1* mutant and control. All assessments were performed from at least three clutches from each mutant. ** $p < 0.01$ by Mann–Whitney *U*-test. Control = eggs from crosses of wildtype females with *vasa::gfp* males; *foxr1* = eggs from crosses of *foxr1* mutant females with *vasa::gfp* males.

Full-size DOI: 10.7717/peerj.5534/fig-4

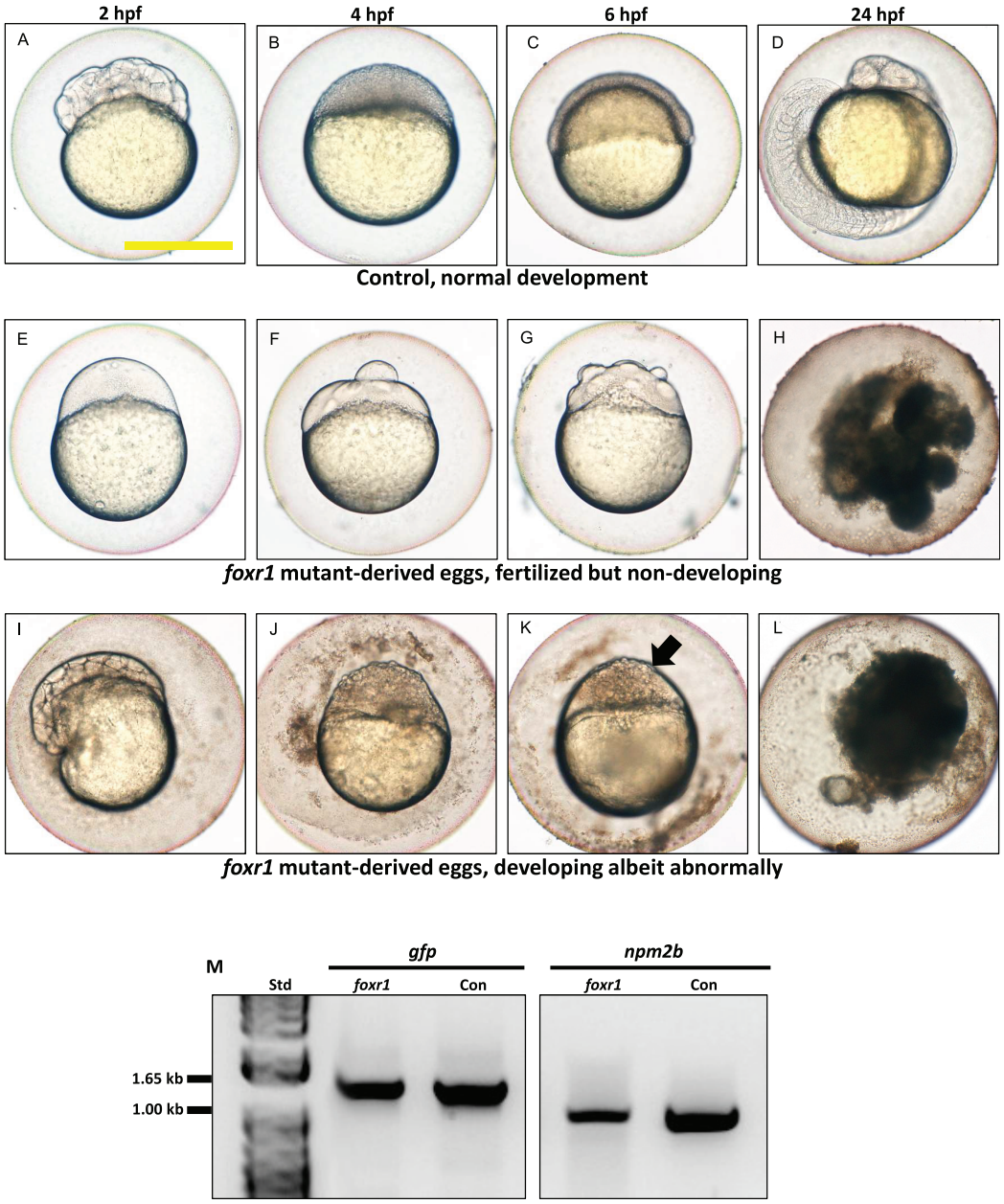

Figure 5 Effect of *foxr1* deficiency on zebrafish embryogenesis. Representative images demonstrating development of fertilized eggs from crosses between control (A–D) and *foxr1* (E–L) females and *vasa::gfp* males from 2 to 24 h post-fertilization (hpf). In the control eggs, the embryos were at 64-cell (A), oblong (B), germ ring (C), and 24-somite (D) stages according to Kimmel et al. (1995). Eggs from *foxr1* mutant females were non-developing with a non-cellularized morphology (E–H) or developing with an abnormal morphology (I–L). (A, E, I) = images taken at two hpf; (B, F, J) = images taken at four hpf; (C, G, K) = images taken at six hpf; (D, H, L) = images taken at 24 hpf. Scale bar denotes 500 μm. The arrow demonstrates an abnormally cellularized blastodisc that was sitting atop an enlarged syncytium. (M) Genotypic analysis of the eggs from crosses of *foxr1* mutant females and *vasa::gfp* males to determine fertilization status. The *gfp* and *vasa* primers produced a band that was 1,333 base pairs in size. Detection of the *npm2b* gene (band size = 850 base pairs) was used as a control. Con = eggs from crosses of wildtype females with *vasa::gfp* males; *foxr1* = eggs from crosses of *foxr1* mutant females with *vasa::gfp* males. $N = 5$ each for *foxr1* mutant and control. Full-size DOI: 10.7717/peerj.5534/fig-5

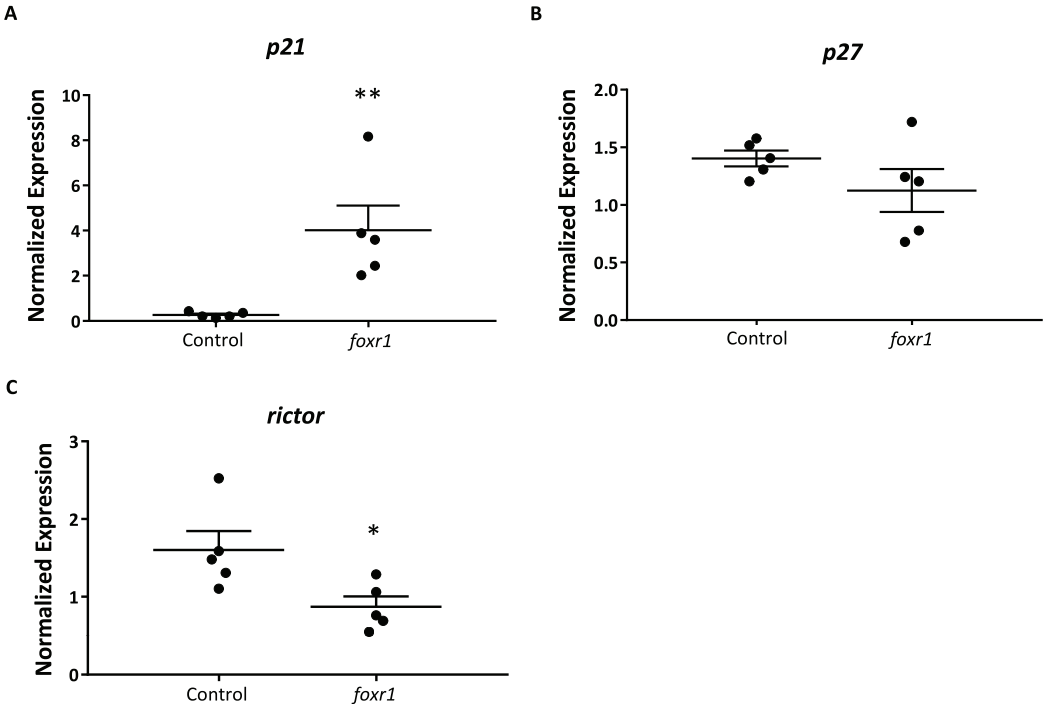

Figure 6 Expression profiles of (A) *p21*, (B) *p27*, and (C) *rictor* in eggs from *foxr1* mutant females. Fertilized eggs from *foxr1* mutant females were subjected to qPCR for examination of the transcript levels of *p*21, *p*27, and *rictor*. The graphs demonstrate representative data from a single clutch from a mutant female. Data were normalized to *18*S, β-*actin*, and *ef1*α. $N = 4$ each for *foxr1* mutant and control, at least two clutches were used from each animal, and each experiment was performed in duplicate. $^{*}p < 0.05$, $^{**}p < 0.01$ by Mann–Whitney *U*-test. Full-size DOI: 10.7717/peerj.5534/fig-6

(Fig. 4B). The frequency of the mutation in the mutant females is demonstrated in Fig. 4C, and it was observed that three of the mutants produced abundant non-developing eggs that remained non-cellularized, reflecting their failure to undergo cell division (Figs. 5E–5H). The eggs derived from these three *foxr1* mutant females (Fig. 4: *foxr1-1, foxr1-2, and fox1-3*) did not undergo any cell division at two hpf and continued to display a complete lack of development up to eight hpf. By 24 hpf, these non-developing eggs that failed to divide were all dead. In addition, two of the mutants (Fig. 4: *foxr1-4 and fox1-5*) produced developmentally incompetent eggs with two phenotypes; those with a non-cellularized morphology (Figs. 5E–5H), and another population that developed albeit with an abnormal morphology (Figs. 5I–5L). These fertilized and developing embryos were structurally abnormal, with unsmooth and irregularly-shaped yolk as well as asymmetrical cell division that culminated into a blastodisc with a group of cells on top of an enlarged syncytium (Fig. 5K, arrow). These eggs underwent developmental arrest at around four hpf or the MBT and appeared to regress with further expansion of the syncytium (Figs. 5J–5K) until death by 24 hpf.

The observed phenotype of the *foxr1* mutant-derived uncellularized eggs was very similar to previously described unfertilized eggs (*Dekens et al., 2003*). Thus, the foxR1 mutant females were mated with *vasa::gfp* males, and the genotype of their progeny was assessed for the presence of the *gfp* gene, which would only be transmitted from the

father since the mutant females did not carry this gene. We found that these uncellularized eggs from the *foxr1* mutant females did indeed carry the *gfp* gene (Fig. 5M), which indicated that some or all of them were fertilized, but were arrested from the earliest stage of development and did not undergo any cell division. These novel findings showed for the first time that *foxr1* is essential for the developmental competence of zebrafish eggs, and is therefore a crucial maternal-effect gene.

In order to delve into the possible mechanisms that may be involved in the reduced reproductive success of the *foxr1* mutants, we investigated the expression levels of *p21*, *p27*, and *rictor*, which were previously reported to be repressed by the Foxr1 transcription factor in mice (*Santo et al., 2012*). We found that there was substantially increased expression of *p21* (4.82 ± 1.09 vs. 0.25 ± 0.04 in controls; $p < 0.002$) while that of *rictor* was significantly decreased (0.87 ± 0.13 vs. 1.60 ± 0.25 in controls; $p < 0.01$) in the *foxr1* mutant-derived eggs as compared to eggs produced by wildtype females (Figs. 6A–6C). The expression of *p27* was unchanged between the two groups. These results were in line with the growth arrested phenotype that was observed in the uncellularized and developmentally challenged eggs from the *foxr1* mutant females.

DISCUSSION

In this study, we first investigated the evolutionary history of *foxr1* in order to gain perspective into its phylogenetic relationship among homologs from a wide range of species and to clarify its origins. Using the zebrafish protein sequence as query to search for homologs in other species, we retrieved Foxr1 sequences from a broad variety of vertebrates, including actinopterygii, sarcopterygii, and sauropsids which suggested the importance of this protein in most vertebrates. We also retrieved Foxr2 sequences from many vertebrates due to its high similarity to the zebrafish Foxr1 peptide (Data S3), although we and others demonstrated that the *foxr2* gene is absent from all actinopterygii and sauropsid species, and can only be found in mammals. Evidence from the phylogenetic analyses showed a clear distinction in derivation of the actinopterygian *foxr1* and the mammalian *foxr2;* the divergence of the ancestral *foxr1* gene in actinopterygii from that of the sarcopterygii and sauropsids occurred quite early in evolution, while the divergence of mammalian *foxr1* and *foxr2* is a much more recent event (Fig. 1). Further, the synteny analysis (Fig. 2) showed that there was much conservation of genomic synteny surrounding the *foxr1* loci between the basal actinopterygian, spotted gar, and actinopterygii and sauropsids, while the neighboring loci around the *foxr2* were completely different in comparison to those next to *foxr1* which suggested that *foxr2* originated from a recent gene duplication or transposition event as previously proposed (*Katoh & Katoh, 2004a*). We also found that in a small subset of species [rainbow trout (*Oncorhynchus mykiss*) and brook trout (*Salvelinus fontinalis*), as well as northern pike (*Esox lucius*), cod (*Gadus morhua*), medaka (*Oryzias latipes*), and spotted gar (*Lepisosteus oculatus*)], two Foxr1 sequences were observed. This suggested that independent gene duplication events occurred in these lineages. It is also possible that *foxr1* was duplicated in the ancestral actinopterygii followed by the loss of one copy in a lineage-dependent manner. Finally, it appeared that the different whole-genome duplication events, the teleost-specific

genome duplication and salmonid-specific genome duplication did not impact the current *foxr1* gene diversity because in most species, only one *foxr1* gene was retained. The presence of two *foxr1* sequences in the above-mentioned species could also be due to independent and phylum-specific gene retention or independent gene duplication events that occurred only in these species or technical differences due to different sequencing procedures. Further phylogenetic, synteny, and functional analyses on the two copies of *foxr1* in these species are warranted in order to verify the functionality of both genes.

The essentialness of *foxr1* was suggested by the wide-ranging presence of this gene in most vertebrates and the retention of a single copy in most teleosts despite multiple whole genome duplication events, but its biological function is still largely unknown. Previous reports have demonstrated the predominant expression of *foxr1* mRNA in the ovary of medaka, eel, and tilapia (*Yuan et al., 2014*; *Geffroy et al., 2016*; *Lai et al., 2015*), but it was found mostly in the male germ cells and spermatids in mouse and human (*Petit et al., 2015*). It was further shown to be abundantly expressed in the early cleavage and gastrula stages of Xenopus embryos, but absent in post-gastrula stages due to rapid degradation of its mRNA, indicating that it is a maternally-inherited transcript (*Schuff et al., 2006*). Thus, the *foxr1* gene may play different roles in reproduction in teleost fish/amphibians and mammals, suggesting that *foxr2* in mammals may have evolved to have comparable functions to the teleost/amphibian *foxr1* while mammalian *foxr1* is mostly involved in male reproduction and development. Of note, the mammalian *foxr2* is thus far observed only on the X chromosome highly indicating a function in female reproduction (Fig. 2). Future studies to test this are necessary to confirm the function of *foxr2.* To confirm these results found in other teleosts in zebrafish, we first examined the expression profile of *foxr1* in various tissues, and we showed by qPCR as well as by RNA-seq that there was also an ovarian-specific expression of *foxr1* and negligible amount in the testis as in the other fish species. By ISH, we found that the *foxr1* transcript was progressively stored in the growing oocytes from the very early stages (Figs. 3C–3D, arrows) to later staged oocytes (Figs. 3D–3E), and could be found abundantly in mature fertilized eggs (Figs. 3B and 4A). These results demonstrated that *foxr1* is one of the maternal products that is deposited into the developing oocytes during oogenesis in zebrafish as observed in other fish species. These findings suggest that *foxr1* may function as a maternal-effect gene such as *npm2a*, *npm2b* (*Cheung et al., 2017*), *bucky ball* (*Bontems et al., 2009*), *futile cycle* (*Lindeman & Pelegri, 2012*), and *wnt* (*Nicol & Guiguen, 2011*).

In recent years, there has been an increasing identification of maternal-effect genes and their functions, but there is still limited information on the role of genes that regulate early embryogenesis. Previous studies have found that *irreducible*, *indivisible*, *atomos*, *cellular island*, *cellular atoll*, and *nebel* genes among others have roles in early embryonic cell cleavage and cell division, but their protein identity as well as their regulatory mechanisms are largely unknown or not yet clarified (*Dosch et al., 2004*; *Pelegri et al., 1999*). Having established that *foxr1* was indeed a maternal factor, we investigated its function via mutagenic analysis with CRISPR/cas9. We used the F0 mosaic mutant females that were shown to have a decreased level of *foxr1* mRNA for analysis due to the difficulty in transmitting the mutated *foxr1* gene to future generations as both the F0 *foxr1* mutant

females and males produced mostly non-viable progeny, and the surviving descendants were all of wildtype genotype. We found that the *foxr1* mutant females produced bad quality eggs, and the developmental success of their progeny was very low, similar to that of *foxl2* and *foxo3* mutants. These latter two genes have been previously shown to be crucial in ovarian determination since they are necessary for the development of the ovary as well as ovarian fate maintenance via suppression of male cues (*Bertho et al., 2016*; *Hosaka et al., 2004*). Deficiency in either of these two genes results in small ovaries and disorganized follicles that cannot mature as well as the appearance of testis-specific cells. Thus, it is possible that *foxr1* may be also required for proper ovarian development and function, as also observed for *foxl2* and *foxo3* mutants, and further histological analysis on ovaries from the *foxr1* mutants is warranted. In addition, we found that the *foxr1* mutant-derived eggs were non-cellularized and did not undergo subsequent cell division despite being fertilized, as also observed for eggs derived from *npm2b* mutant females (*Cheung et al., 2017*). This suggested that their defect did not lie in the capability to be fertilized, as seen in *slc29a1a* and *otulina* mutants (*Cheung et al., 2018*), but in the cell cycle and proliferation processes. Thus, we investigated the expression profiles of *p21*, *p27*, and *rictor*, which are all cell cycle and cell survival regulators, since *Santo et al. (2012)* had previously knocked down *foxr1* using short hairpin RNAs in mammalian cells and found it to be a transcriptional repressor of them. In this report, we also observed a dramatic increase in *p21* transcript in the eggs from *foxr1* mutant females, although the expression of *p27* was unchanged, while that of *rictor* was decreased. Both *p21* and *p27* are well known cell cycle inhibitors, and *rictor* is a component of the mTOR (mammalian target of rapamycin) complex that is a major regulator of cell growth and proliferation (*Tateishi et al., 2012*; *Peponi et al., 2006*). In fact, mitogens or some survival signal activates a survival cascade, such as the PI3K/Akt pathway, which is activated by the rictor-mTOR complex and promotes cell growth through repression of the negative cell cycle modulators, including *p21* and *p27* (*Sarbassov, Ali & Sabatini, 2005*). Thus, our findings were in line with a phenotype of growth arrest and anti-proliferative effects as seen in our eggs derived from *foxr1* mutant females. The different results that we observed as compared to those from Santo et al. were probably due to species- and cell type-specific effects.

In this study, we showed that *foxr1* is found in a wide-range of vertebrates and is homologous to the *foxr1* genes found in other species. In teleosts, *foxr1* expression is found predominately in the ovary while in mammals, it appears to be specific to the male germline (*Petit et al., 2015*). We also found that *foxr1* is a novel maternal-effect gene and is highly expressed in the developing oocytes as well as accumulated in mature eggs to be used in early embryogenesis. Our findings suggest that maternally-inherited *foxr1* may be required for the first few cleavages after fertilization for proper cell growth and proliferation possibly via *p21* and *rictor*, since deficiency in *foxr1* leads to either complete lack of or abnormal cell division culminating to early death in the fertilized egg. Further molecular analyses to disrupt *p21* and *rictor* expression in *foxr1* mutants to investigate their function in these mutants are necessary. Thus, the results of this study are the first to establish a link between egg quality, the control of early cell cycle, and the molecular regulatory mechanisms via the potential transcriptional regulator, FoxR1.

CONCLUSIONS

Our study shows for the first time that *foxr1* is an essential maternal-effect gene and is required for proper cell division and survival possibly via the p21 and mTOR pathways. These novel findings will broaden our knowledge on the functions of specific maternal factors stored in the developing egg and the underlying mechanisms that contribute to reproductive fitness.

ACKNOWLEDGEMENTS

The authors would like to thank all the members of the LPGP laboratory for their assistance. We thank JJ Lareyre for the use of the *vasa::gfp* males for the fertilization assays.

ADDITIONAL INFORMATION AND DECLARATIONS

Funding

This work was supported by the French National Research Agency ANR (Maternal Legacy ANR-13-BSV7-0015) and by Région Bretagne. The funders had no role in study design, data collection and analysis, decision to publish, or preparation of the manuscript.

Grant Disclosures

The following grant information was disclosed by the authors:
French National Research Agency ANR: Maternal Legacy ANR-13-BSV7-0015.

Competing Interests

The authors declare that they have no competing interests.

Author Contributions

- Caroline T. Cheung conceived and designed the experiments, performed the experiments, analyzed the data, prepared figures and/or tables, authored or reviewed drafts of the paper, approved the final draft.
- Amélie Patinote performed the experiments, approved the final draft.
- Yann Guiguen conceived and designed the experiments, approved the final draft.
- Julien Bobe conceived and designed the experiments, analyzed the data, authored or reviewed drafts of the paper, approved the final draft.

Animal Ethics

The following information was supplied relating to ethical approvals (i.e., approving body and any reference numbers):

Protocols were approved by the Rennes ethical committee for animal research (CREEA) under approval no. R2012-JB-01.

Data Availability

The following information was supplied regarding data availability:

The raw data are provided in the Supplemental Files.

Supplemental Information

Supplemental information for this article can be found online at http://dx.doi.org/10.7717/peerj.5534#supplemental-information.

REFERENCES

Auer TO, Duroure K, De Cian A, Concordet JP, Del Bene F. 2014. Highly efficient CRISPR/cas9-mediated knock-in in zebrafish by homology-independent DNA repair. *Genome Research* **24(1)**:142–153 DOI 10.1101/gr.161638.113.

Baroux C, Autran D, Gillmor CS, Grimanelli D, Grossniklaus U. 2008. The maternal to zygotic transition in animals and plants. *Cold Spring Harbor Symposia on Quantitative Biology* **73**:89–100 DOI 10.1101/sqb.2008.73.053.

Bertho S, Pasquier J, Pan Q, Le Trionnaire G, Bobe J, Postlethwait JH, Pailhoux E, Schartl M, Herpin A, Guiguen Y. 2016. Foxl2 and its relatives are evolutionary conserved players in gonadal sex differentiation. *Sexual Development* **10(3)**:111–129 DOI 10.1159/000447611.

Bontems F, Stein A, Marlow F, Lyautey J, Gupta T, Mullins MC, Dosch R. 2009. Bucky ball organizes germ plasm assembly in zebrafish. *Current Biology* **19(5)**:414–422 DOI 10.1016/j.cub.2009.01.038.

Cheung CT, Nguyen T, Le Cam A, Patinote A, Journot L, Reynes C, Bobe J. 2018. Lost in translation: egg transcriptome reveals molecular signature to predict developmental success and novel maternal-effect genes. *biorxiv preprint* 286815 DOI 10.1101/286815.

Cheung CT, Pasquier J, Bouleau A, Nguyen T-V, Chesnel F, Guiguen Y, Bobe J. 2017. Double maternal effect: duplicated nucleoplasmin 2 genes, npm2a and npm2b, are shared by fish and tetrapods, and have distinct and essential roles in early embryogenesis. *biorxiv preprint* 104760 DOI 10.1101/104760.

Chi W, Gao Y, Hu Q, Guo W, Li D. 2017. Genome-wide analysis of brain and gonad transcripts reveals changes of key sex reversal-related genes expression and signaling pathways in three stages of *Monopterus albus*. *PLOS ONE* **12(3)**:e0173974 DOI 10.1371/journal.pone.0173974.

Dekens MPS, Pelegri FJ, Maischein HM, Nusslein-Volhard C. 2003. The maternal-effect gene futile cycle is essential for pronuclear congression and mitotic spindle assembly in the zebrafish zygote. *Development* **130(17)**:3907–3916 DOI 10.1242/dev.00606.

Dereeper A, Audic S, Claverie JM, Blanc G. 2010. BLAST-EXPLORER helps you building datasets for phylogenetic analysis. *BMC Evolutionary Biology* **10(1)**:8–13 DOI 10.1186/1471-2148-10-8.

Dereeper A, Guignon V, Blanc G, Audic S, Buffet S, Chevenet F, Dufayard JF, Guindon S, Lefort V, Lescot M, Claverie JM, Gascuel O. 2008. Phylogeny.fr: robust phylogenetic analysis for the non-specialist. *Nucleic Acids Research* **36(Web Server)**:W465–W469 DOI 10.1093/nar/gkn180.

Dosch R, Wagner DS, Mintzer KA, Runke G, Wiemelt AP, Mullins MC. 2004. Maternal control of vertebrate development before the midblastula transition: mutants from the zebrafish I. *Development Cell* **6**:771–780.

Gagnon JA, Valen E, Thyme SB, Huang P, Akhmetova L, Pauli A, Montague TG, Zimmerman S, Richter C, Schier AF. 2014. Efficient mutagenesis by cas9 protein-mediated oligonucleotide insertion and large-scale assessment of single-guide RNAs. *PLOS ONE* **9(5)**:e98186 DOI 10.1371/journal.pone.0098186.

Geffroy B, Guilbaud F, Amilhat E, Beaulaton L, Vignon M, Huchet E, Rives J, Bobe J, Fostier A, Guiguen Y, Bardonnet A. 2016. Sexually dimorphic gene expressions in eels: useful markers for early sex assessment in a conservation context. *Scientific Reports* **6(1)**:34041 DOI 10.1038/srep34041.

Hannenhalli S, Kaestner KH. 2009. The evolution of Fox genes and their role in development and disease. *Nature Reviews Genetics* **10(4)**:233–240 DOI 10.1038/nrg2523.

Hosaka T, Biggs WH, Tieu D, Boyer AD, Varki NM, Cavenee WK, Arden KC. 2004. Disruption of forkhead transcription factor (FOXO) family members in mice reveals their functional diversification. *Proceedings of the National Academy of Sciences of the United States of America* **101(9)**:2975–2980 DOI 10.1073/pnas.0400093101.

Katoh M, Katoh M. 2004a. Germ-line mutation of Foxn5 gene in mouse lineage. *International Journal of Molecular Medicine* **14(3)**:463–467 DOI 10.3892/ijmm.14.3.463.

Katoh M, Katoh M. 2004b. Identification and characterization of human FOXN6, mouse Foxn6, and rat Foxn6 genes in silico. *International Journal of Oncology* **25(1)**:219–223 DOI 10.3892/ijo.25.1.219.

Kimmel CB, Ballard WW, Kimmel SR, Ullmann B, Schilling TF. 1995. Stages of embryonic development of the zebrafish. *Developmental Dynamics* **203(3)**:253–310 DOI 10.1002/aja.1002030302.

Lai KP, Li JW, Wang SY, Chiu JMY, Tse A, Lau K, Lok S, Au DWT, Tse WKF, Wong CKC, Chan TF, Kong RYC, Wu RSS. 2015. Tissue-specific transcriptome assemblies of the marine medaka *Oryzias melastigma* and comparative analysis with the freshwater medaka *Oryzias latipes*. *BMC Genomics* **16(1)**:135 DOI 10.1186/s12864-015-1325-7.

Lindeman RE, Pelegri F. 2010. Vertebrate maternal-effect genes: insights into fertilization, early cleavage divisions, and germ cell determinant localization from studies in the zebrafish. *Molecular Reproduction and Development* **77(4)**:299–313 DOI 10.1002/mrd.21128.

Lindeman RE, Pelegri F. 2012. Localized products of futile cycle/lrmp promote centrosome-nucleus attachment in the zebrafish zygote. *Current Biology* **22(10)**:843–851 DOI 10.1016/j.cub.2012.03.058.

Mahlapuu M, Ormestad M, Enerback S, Carlsson P. 2001. The forkhead transcription factor Foxf1 is required for differentiation of extra-embryonic and lateral plate mesoderm. *Development* **128(2)**:155–166.

Mali P, Yang L, Esvelt KM, Aach J, Guell M, Dicarlo JE, Norville JE, Church GM. 2013. RNA-guided human genome engineering via cas9. *Science* **339(6121)**:823–826 DOI 10.1126/science.1232033.

Martins R, Lithgow GJ, Link W. 2016. Long live FOXO: unraveling the role of FOXO proteins in aging and longevity. *Aging Cell* **15(2)**:196–207 DOI 10.1111/acel.12427.

Nicol B, Guiguen Y. 2011. Expression profiling of Wnt signaling genes during gonadal differentiation and gametogenesis in rainbow trout. *Sexual Development* **5(6)**:318–329 DOI 10.1159/000334515.

Pasquier J, Cabau C, Nguyen T, Jouanno E, Severac D, Braasch I, Journot L, Pontarotti P, Klopp C, Postlethwait JH, Guiguen Y, Bobe J. 2016. Gene evolution and gene expression after whole genome duplication in fish: the PhyloFish database. *BMC Genomics* **17(1)**:368 DOI 10.1186/s12864-016-2709-z.

Pelegri F, Knaut H, Maischein H-M, Schulte-Merker S, Nüsslein-Volhard C. 1999. A mutation in the zebrafish maternal-effect gene nebel affects furrow formation and vasa RNA localization. *Current Biology* **9(24)**:1431–1440 DOI 10.1016/s0960-9822(00)80112-8.

Peponi E, Drakos E, Reyes G, Leventaki V, Rassidakis GZ, Medeiros LJ. 2006. Activation of mammalian target of rapamycin signaling promotes cell cycle progression and protects cells from apoptosis in mantle cell lymphoma. *American Journal of Pathology* **169(6)**:2171–2180 DOI 10.2353/ajpath.2006.051078.

Petit FG, Kervarrec C, Jamin SP, Smagulova F, Hao C, Becker E, Jégou B, Chalmel F, Primig M. 2015. Combining RNA and protein profiling data with network interactions identifies genes associated with spermatogenesis in mouse and human1. *Biology of Reproduction* **92(3)**:1–18 DOI 10.1095/biolreprod.114.126250.

Sander JD, Maeder ML, Reyon D, Voytas DF, Joung JK, Dobbs D. 2010. ZiFiT (Zinc Finger Targeter): an updated zinc finger engineering tool. *Nucleic Acids Research* **38(Web Server)**:W462–W468 DOI 10.1093/nar/gkq319.

Santo EE, Ebus ME, Koster J, Schulte JH, Lakeman A, Van Sluis P, Vermeulen J, Gisselsson D, Øra I, Lindner S, Buckley PG, Stallings RL, Vandesompele J, Eggert A, Caron HN, Versteeg R, Molenaar JJ. 2012. Oncogenic activation of FOXR1 by 11q23 intrachromosomal deletion-fusions in neuroblastoma. *Oncogene* **31(12)**:1571–1581 DOI 10.1038/onc.2011.344.

Sarbassov DD, Ali SM, Sabatini DM. 2005. Growing roles for the mTOR pathway. *Current Opinion in Cell Biology* **17(6)**:596–603 DOI 10.1016/j.ceb.2005.09.009.

Schuff M, Rossner A, Donow C, Knochel W. 2006. Temporal and spatial expression patterns of FoxN genes in *Xenopus laevis* embryos. *International Journal of Developmental Biology* **50(4)**:429–434 DOI 10.1387/ijdb.052126ms.

Tateishi Y, Matsumoto A, Kanie T, Hara E, Nakayama K, Nakayama KI. 2012. Development of mice without Cip/Kip CDK inhibitors. *Biochemical and Biophysical Research Communications* **427(2)**:285–292 DOI 10.1016/j.bbrc.2012.09.041.

Yilmaz O, Patinote A, Thao T, Nguyen TV, Com E, Lavigne R, Pineau C, Sullivan CV, Bobe J. 2017. Scrambled eggs: proteomic portraits and novel biomarkers of egg quality in zebrafish (*Danio rerio*). *PLOS ONE* **12(11)**:e0188084 DOI 10.1371/journal.pone.0188084.

Yuan J, Tao W, Cheng Y, Huang B, Wang D. 2014. Genome-wide identification, phylogeny, and gonadal expression of fox genes in Nile tilapia, *Oreochromis niloticus*. *Fish Physiology and Biochemistry* **40(4)**:1239–1252 DOI 10.1007/s10695-014-9919-6.